Steady state and Dynamic simulation of molten carbonate fuel cells.

M. Fermeglia[(1)(2)], A. Cudicio[(1)], G. DeSimon[(1)], G. Longo [(2)], S. Pricl[(1)]
[1] DICAMP, University of Trieste, Piazzale Europa 1, 34127 Trieste, Italy
[2] ICS-UNIDO, Area Science Park, Padriciano, Trieste, Italy

This paper addresses the simulation of fuel cells systems in steady state and in dynamic condition. Two models are developed to this aim: (i) a steady state models implemented in Aspen+ 11.1 simulating a global carbonate fuel cells (MCFC) power plant and (ii) a dynamic model implemented in Aspen Custom Modeler for the same cell. Both models are based on real plant data, and the simulation parameters are selected according to real operating conditions. The process studied is a 500 kW MCFC power system based on Ansaldo fuel cells (AFC) technology. The steady state simulation evidenced the main interactions among the different devices composing the process, and the sensitivity analysis conducted showed that there is room for improvement in electrical efficiency by increasing the steam to methane ratio, the pressure and the feed air. The dynamic simulation has shown the quantitative response of the system to several disturbances and proved to be a valid tool for determining the temperature, the current and the voltage profiles as a function of time within the fuel cells.

1. Introduction

Fuel cells are high efficiency and low polluting electrochemical devices, meant to convert the hydrogen chemical energy into electrical energy. Many are the intervening parameters for defining the optimum process condition and its stability with respect to possible external perturbation. It is therefore important to simulate the process for different steady state conditions for determining the best process parameters and study the effect of process modification with respect to efficiency and energy production. It is also very interesting to study the dynamic behaviour of the process for determining the time dependency of key process parameters for system changes.

Among the different fuel cells developed so far, molten carbonate fuel cells (MCFC), also referred to as “second generation” cells (Kraaij et al., 1998), have been deeply investigated in the last decade. Accordingly, MCFC dynamic simulation may be helpful in the further development before commercialization (Bishoff and Huppman, 2002).

In fuel cells, and in MCFC in particular, high global efficiency with respect to other electrical energy production systems can be reached thanks to many contributory causes, detailed reviewed by De Simon et al. (2003). A MCFC plant integrates a stack with preceding cycles of fuel conditioning and following operations of residual energy recover. Fig. 1 shows the essential geometry of a single cell (right) and the general process for energy production (left).

The main components of the MCFC are: (i) two metal current collectors, whose task is also to distribute the gas streams across the electrodes surfaces; (ii) a NiO-based porous

cathode, where the reduction reaction occurs, producing the $CO_3^{\ 2}$ ion, that must travel across an (iii) electrolyte tile (made up by molten K, Na and Li carbonates in a solid porous and inert matrix) and reach a (iv) Ni-based porous anode, where oxidation occurs. The total reaction is essentially the hydrogen combustion reaction combined with a CO_2 transfer from cathode to anode.

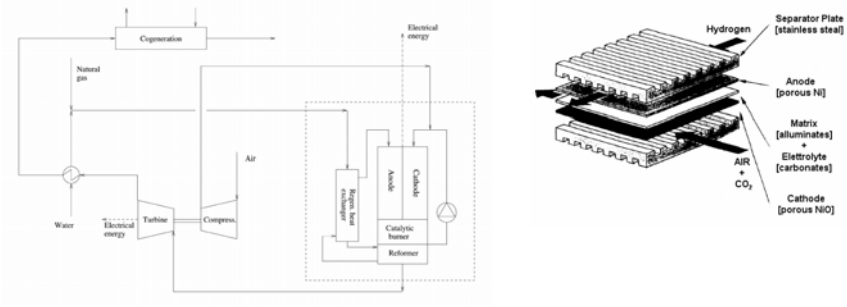

Figure 1: MCFC Process (left) and details of the fuel cell (right)

2. Model Development

2.1 Steady state model

The steady state simulation model is based on the approach of Arato et al. (2001).The local behavior is described as a simple electrical circuit, series of an ideal voltage, determined by the Nernst equation, and an internal resistance, made up by the sum of the three contributions: contact resistance (R_c) between electrode and current, collector, electrolyte tile Ohmic resistance (R_e) and polarization contribution (R_p). The first term was found to be simply a constant, the second term is an exponential function of temperature and the last one depends on both temperature and partial pressures of the species involved in the electrochemical reaction. All coefficients of this model are obtained by experimental data fittings.

The main assumptions considered in the model development are (i) steady state conditions; (ii) the anodic electrochemical reaction was neglected for its very low rate; (iii) non-limiting diffusion in macro-pores of the electrode and in gas stream; (iv) current collector as an ideal conductor (constant voltage on whole surface); (v) adiabatic conditions; (vi) water gas-shift reaction considered at the equilibrium for its high rate; (vii) ideal gas. It is important to note that diffusion phenomena occur at high reactants utilization and reduce heavily the device efficiency; for this reason they must be avoided, by defining the cell working conditions in terms of gas utilization such as diffusion is negligible. So assumption (iii) is justified.

The model considers local temperature, pressure and composition changes along gases path in the ducts, because of reactions, heat transfer and pressure drop. To find global cell behavior it is necessary to solve simultaneously four sets of equations: mass balance (for each gas component), momentum balance (of cathode and anode gas streams),

energy balance and local kinetics. The boundary conditions are input gas streams temperature, pressure and composition, and the assumption of adiabatic conditions. For the numerical solution, finite difference and relaxation methods have been employed and implemented in Fortran 90 language.

The process simulation was performed by Aspen plus ™. Default Aspen plus™ models have been used for traditional plant units, while for fuel cells stack a custom Fortran 90 code was developed. The general process scheme simulated in this work is reported in fig. 2. Details of the model implementation of the single units and the global process can be found in De Simon et al. (2003).

2.2 Dynamic model

The chemical-physical fundamental equations are organized to give an easily solvable system which integrates fluid dynamic and reaction equations, solving the system in an equation oriented approach. Equations are grouped in modules thus allowing simple and fast modifications for screening many different configurations. Chemical reactions are coupled with homogeneous and heterogeneous heat and mass transport phenomena. A fully distributed bi-dimensional open loop model was implemented in the commercial process simulator ACM (AspenTech™). The dynamic model for a MCFC was developed, starting from general balances adapted to the specific case; the equations approximating the real physical device were grouped in a system of a considerable dimension (16.996 variables) solved with an PC (850 MHz and 512 MB Ram) in a reasonable time (10 min for a 40 h run). Details of the derivation of the model can be found in Cudicio (2003).

3. Results and Discussion

Fuel cells efficiency is defined as the ratio of electric power produced by the stack and chemical power of the fuel actually consumed. Referring the efficiency to total input fuel energy could be misleading because residual fuel is doubly recovered. In the catalytic burner part of the heat produced is transferred to the reformer, where it is converted to chemical energy by means of endothermic reactions; another part of gas energy is next recovered in the turbine. These two energy recovers take place with less efficiency than fuel cell conversion. Hence, to achieve high global efficiency, it is useful to assign most possible energy to electrochemical conversion. The process can be considered a fuel cell/gas turbine hybrid cycle (FC/GT), where topping cycle is FC and bottoming one is GT. It is useful considering the variables that affect bottoming cycle behavior. For a gas turbine system the efficiency is improved by high pressure ratio and high turbine input gas temperature. In the present case, FC and MIR substitute the combustion chamber, but the qualitative trend remains unchanged.

3.1 Steady state and sensitivity analysis

Simulations start with a ‘‘base case’’ in which all the assumptions are used as preliminary project specifications. The input Nusselt local Number is adjusted so that the calculated results match the literature ones. Base case input specifications and simulation results are reported in table 1. Excellent agreement is obtained when comparing the simulation results with the experimental data measured directly on a pilot plant: a 500 kW MCFC power system based on Ansaldo fuel cells (AFC) technology (Bosio et al., 1998). Process parameters have been varied in the sensitivity analysis.

Input specifications		Base case results	
		CH_4 plant feed rate (kg/h)	82
Cell solid temperature (_C)	650	Stack power (kW)	505.6
Fuel utilisation (%)	75	Bottoming cycle power (kW)	77.5
Oxygen utilisation (%)	30	Thermal cogeneration power (kW)	261
Pressure (bar)	3.5	Reforming temperature (_C)	688
Steam/methane ratio	3	CH_4 conversion (%)	79.3
Steam temperature (_C)	170	Stack efficiency (%)	60.3
		Cell voltage (V)	0.769
		Bottoming cycle efficiency (%)	12.2
		Global process electrical efficiency (%)	51.1
		Cogenerative efficiency (%)	74

Table 1: Input specifications and base case results of steady state simulation of MCFC.

An increase in the steam to methane ratio (the main parameters of the process) results in an improvement of the reforming and gas shift equilibrium, because the amount of one of the reactants is increased. In spite of a slight fuel cells efficiency reduction, due to reactants dilution, the global electrical efficiency improves. The main factors explaining this behavior are (i) more energy is converted in the stack for a higher amount of hydrogen available, (ii) more heat is removed from effluent gas, and so more heat is recycled into the plant and in the bottoming cycle, increasing its efficiency. The effect of pressure on the electrical efficiency has different effects in different part of the plant. The global effect of an increase of pressure shows that the increase of the two cycle efficiencies overcomes methane conversion effect. But there is a worsening of cogeneration, because residual heat exits again in a more degenerated form. The fresh air flow rate does not show any changes of cells, bottoming cycle and co-generative efficiencies but shows a reduction in global electrical efficiency as air flow rate is increased. This fact can be explained in a chain of effects happening inside the process.

3.2 Dynamic simulation

The dynamic simulation model described in this work focuses on the fuel cell as the main component of the process. The validation of the model is done also in this case by comparing the base case results obtained from the dynamic model run at steady state conditions, with those of the previous model. The agreement was excellent. Base case is also validated against literature and experimental data: as examples (Bosio et al., 1999) reports a mean temperature of 932 K (in the case most similar to this one); Mangold and Sheng (2003) report an anode outlet temperature of 658 °C and a cathode outlet temperature of 714 °C; He and Chen (1995) report a hot spot of 710 °C in the same position predicted by our model; references from which we took experimental correlations (Bosio et al., 1999, Koh et al., 2000, Fontes et al., 1995) show a discrete agreement also in distributions and three dimensional diagrams. In the sensitivity analysis, changes have been made aiming at finding which variables have the great impact on the process; attention has been focused on the input temperatures, velocities and mean current density, as well as pressure. The model is tested in transient conditions changing one or more input variables, one at a time or simultaneously, with many different perturbations, at one or both the electrodes; the first steady state

considered, in all the cases, is the base one; after 60 h of simulations the estimated errors were for each variable were around 0.1% or less (Cudicio, 2003).

3.2.1 Pressure effect

A unity loss of pressure at anode (P_A=2.5 bar) is supposed to happen suddenly at time 0.5 h; the variation is obtained working on densities of components but leaving constant molar fractions. Anode temperature drops quickly because of the thermodynamic effect and after rises because of the heat of reaction; the first effect is prevalent, as the temperature becomes smaller than that before the perturbation; this behaviour spreads, by conduction, to the electrolyte and cathode giving an inverse response. Hydrogen utilization falls down because at constant molar fraction there is less hydrogen in input for a given rate of reaction. Utilization has a negative peak because $\rho \sim T^{-1}$ and so there is more H_2 and O_2 for the electrochemical reaction immediately after the perturbation. At the beginning potential rises because, for constant pressure at cathode and same anode partial pressures, V is proportional to $\ln(P_A^{-1}) \sim P_A^{-1}$; at the end the decrease of E_0 with rising temperature predominates. Rising density of carbon monoxide and water follows the equilibrium of the WGS reaction. All the variables distributed on cell plane can be investigated in time evolution; in these cases we can see the presence of an hot spot, in the anode temperature, at steady state, in the corner farthest from input sections, due to the progressive heating of the relatively cold gases at both electrodes. The evolution of the temperature follows the mean output anode temperature. Hydrogen is progressively consumed along anode extension; minimum molar fraction is located near the output of the anode and the input of the cathode, were less hydrogen reacts with more oxygen.

3.2.2 Velocity effect

The anode and cathode velocities are rounded off (v_A=1.0 m/h) and (v_C=6.0 m/h), respectively, to obtain less output hydrogen for bottoming operations and less oxygen utilization. The perturbations are applied at the same time at 0.5 h, with a linear ramp for 1.0 h. Utilizations increase for hydrogen and reduce for oxygen. The distribution of tension on cell plane shows a progressive lowering that is concentrated near the output section of the anode showing a stronger dependence on anode partial pressures than that on cathode partial pressures.

3.2.3 Temperature effect

Temperatures are supposed to vary smoothly, with a semi-sinusoidal shape, at both electrodes with the same intensity (30 K less than the base case) but at different times (0.5 h and 0.75 h respectively) and with different durations (1.0 h and 0.5 h respectively). Mean anode temperature at output section responses to semi-sinusoidal input with a semi-sinusoidal shape; cathode feels the modifications yet started at anode; electrolyte mean temperature follows general decrease.

3.2.4 Current effect

Modern molten carbonate fuel cells work at 1.5 kA/m^2; the model investigates larger current densities of 1.7 kA/m^2 supposing a step at time 0.5 h. Tension, obviously, lowers because polarization grows with current. Reaction velocity quickly rises, with more hydrogen burned; WGS reaches a new equilibrium point with production of H_2 from carbon monoxide and water, that is an endothermic reaction which removes heat lowering anode temperature; this new availability do not offset the consumption and the density of hydrogen lowers, as product's densities rise.

Detailed bi- and tri-dimensional graphs and videos showing the effects described for all the variables considered are available at the authors' web page (www.caslab.units.it).

4. Conclusions

This paper has presented the results of the steady state and dynamic simulation of molten carbonate fuel cells (MCFC). A steady state model of the MCFC has been presented and the results of a global process including all the modules discussed. The dynamic simulation of the same MCFC has been described and the results of the simulation discussed. The steady state simulation of the MCFC has enabled the deep understanding of the electrochemical device behavior, useful for its integration with the other units. The simulation of the plant has evidenced the interactions among the devices. Calculations show that global electrical efficiency surely can be kept easily over 50–55%, derived from about 60% of fuel cells stack and 12% of the bottoming cycle. Cogenerative efficiency in the simulation remains instead within 75%. It was found that if the anode exhaust gas is burned before heat exchange with the reformer, a higher conversion is obtained and the global electric and cogenerative efficiencies rises, respectively, from 51.1 and 74 to 54.8 and 75.6%. These results agree with expectations for similar systems (George, 2000) and predict better performance with respect to results for ambient pressure system without GT integration (Gnann, 2001).
The sensitivity analysis showed that there is still room for improvement in electrical efficiency by increasing steam to methane ratio, pressure and decreasing air feed rate. All these variables, at the same time, cause often the cogeneration worsening.
The dynamic simulation results for the MCFC allows us to conclude that the behaviour of the molten carbonate fuel cell, within an acceptable operating range of variables, is strongly influenced by the input temperatures, but even more by the utilizations and by the mean current density desired, that can produce too high temperatures. The MCFC have a time scale of hours.

5. References

Arato, E., B. Bosio, P. Costa and F. Parodi, 2001, J. Power Sources 102, 74.

Bishoff, M. and G. Huppman, 2002, J. Power Sources 105, 216.

Bosio, B., P. Costamagna and F. Parodi, 1999, Chemical engineering science 54, 2907.

Bosio,B., P. Costamagna, F. Parodi and B. Passalacqua, 1998, J. Power Sources 74,175.

Cudicio, A., 2003, Thesis, University of Trieste, Italy.

De Simon,G., F. Parodi, M. Fermeglia and R. Taccani, 2003, J. Power Sources 115,210.

Fontes, E., M. Fontes and D. Siminsson, 1995, Electrochimica acta 40, 1641.

George, R.A., 2000, J. Power Sources 86, 134.

Gnann, M.,2001, The MTU Fuel Cell Hot Module Cogeneration Unit 250Kee, Abstracts of the VII Grove Fuel Cell Symposium, London, September 2001.

He, W. and Q. Chen, 1995, J. Power Sources 55, 25.

Koh, J.-H., B. S. Kang, and H. C. Lim, 2000, J. Power Sources 91, 161.

Kraaij,G.J., G. Rietveld, R.C. Makkus and J.P.P. Huijsmans, 1998, J. Power Sources 71, 215.

Mangold, M. and M. Sheng, 2003, AIChE's Annual Meeting, 169a.